



HAL
open science

High-relaxivity molecular MRI contrast agent to target Gb3-Expressing cancer cells

Stéphanie Deville-Foillard, Anne Billet, Rose-Marie Dubuisson, Ludger Johannes, Philippe Durand, Frédéric Schmidt, Andreas Volk

► **To cite this version:**

Stéphanie Deville-Foillard, Anne Billet, Rose-Marie Dubuisson, Ludger Johannes, Philippe Durand, et al.. High-relaxivity molecular MRI contrast agent to target Gb3-Expressing cancer cells. *Bioconjugate Chemistry*, 2022, 33 (1), pp.180-193. 10.1021/acs.bioconjchem.1c00531 . hal-03551620

HAL Id: hal-03551620

<https://hal.science/hal-03551620>

Submitted on 7 Nov 2022

HAL is a multi-disciplinary open access archive for the deposit and dissemination of scientific research documents, whether they are published or not. The documents may come from teaching and research institutions in France or abroad, or from public or private research centers.

L'archive ouverte pluridisciplinaire **HAL**, est destinée au dépôt et à la diffusion de documents scientifiques de niveau recherche, publiés ou non, émanant des établissements d'enseignement et de recherche français ou étrangers, des laboratoires publics ou privés.

High relaxivity molecular MRI contrast agent to target Gb₃ expressing cancer cells

Stéphanie Deville-Foillard,^{†,‡,*} Anne Billet,^{†,¶} Rose-Marie Dubuisson,^{||} Ludger Johannes,[†] Philippe Durand,[#] Frédéric Schmidt,[†] Andreas Volk^{‡,§,*}

[†] Institut Curie, PSL University Paris, CNRS UMR3666, INSERM U1143, Cellular and Chemical Biology, 75005 Paris, France.

[‡] Institut Curie, Université Paris-Saclay, CNRS, INSERM, CMIB, 91405 Orsay, France.

[§] Université Paris-Saclay, CEA, CNRS, INSERM, BioMaps, Institut Gustave Roussy, 94800 Villejuif, France.

^{||} Université Paris-Saclay, CEA, CNRS, INSERM, BioMaps, Service Hospitalier Frédéric Joliot, 91401 Orsay, France.

[#] Université Paris-Saclay, CNRS UPR 2301, Institut de Chimie des Substances Naturelles, 91198 Gif-sur-Yvette, France.

[¶] Université de Paris, F-75005 Paris, France.

KEYWORDS Targeted contrast agent, Molecular imaging, Protein conjugates, Gadolinium, MRI.

ABSTRACT: Targeted contrast agents can improve magnetic resonance imaging (MRI) for accurate cancer diagnosis. In this work, we used the Shiga toxin B-subunit (STxB) as a targeting agent, which binds to Gb₃, a glycosphingolipid highly overexpressed at the surface of tumor cells. We developed STxB-targeted MRI probes from cyclic peptide scaffold functionalized with 6 to 9 monoamide DO₃A[Gd(III)] chelates. The influence of structural constraints on the longitudinal relaxivity (r_1) of the contrast agents has been studied. The cyclic peptide carrying 9 monoamide DO₃A[Gd(III)] exhibited a r_1 per compound of 32 mM⁻¹s⁻¹ and 93 mM⁻¹s⁻¹ at 9.4 T and 1.5 T respectively. Its conjugation to the pentameric STxB protein led to a 70 kDa compound with a higher r_1 of 150 mM⁻¹s⁻¹ and 475 mM⁻¹s⁻¹ at 9.4 T and 1.5 T respectively. Specific accumulation and cellular distribution of this conjugate in Gb₃ expressing cancer cells were demonstrated using immunofluorescence microscopy and quantified by ICP-MS dosage of Gd(III). Such agent should enable the *in vivo* detection by MRI of tumors expressing Gb₃ receptors.

INTRODUCTION

Tumor specific delivery of potent anticancer drugs is a primary goal of cancer therapy research. Indeed, delivery of high dose of drug specifically to the tumor allows reducing systemic toxicity. Tumor targeting can be achieved using delivery vectors that target receptors overexpressed in cancer cells and accumulate in tumors together with their drug payload. However, due to heterogeneity of tumors and patients, such strategies need to be combined with suitable imaging before or during therapy to estimate in individual subjects and tumors the actual level and distribution of the targeted receptor. This can be achieved through imaging using contrast agents conjugated to the vector.¹ In this work, we used the Shiga toxin B-subunit as a tumor targeted vector. The parental Shiga toxin is produced by intestinal pathogens, *Shigella dysenteriae*, and some pathogenic strains of *E. Coli*.²⁻³ It belongs to the class of AB₅ toxins, formed by the assembly of a toxic catalytic A-subunit that inhibits protein biosynthesis, and a nontoxic homopentameric B-subunit (STxB)⁴ that is responsible for the binding to the

glycosphingolipid globotriaosyl ceramide Gb₃.⁵ Overexpression of the receptor Gb₃ has been reported in human cancers⁶ such as Burkitt's and centrofollicular lymphomas⁷⁻⁸ and in a wide range of solid tumors such as breast⁹⁻¹⁰, ovarian¹¹, pancreatic¹², colon¹³⁻¹⁴, gastric¹⁵, testicular tumors¹⁶, and tumor neovasculature.¹⁷⁻¹⁸ STxB can therefore be used as a vector for image-guided targeted tumor therapy.¹⁹⁻²¹ After binding to Gb₃, STxB is endocytosed and follows the retrograde route from the plasma membrane to the endoplasmic reticulum *via* early endosomes and the Golgi apparatus.²¹⁻²³ Unlike the endosomal-lysosomal route taken classically by antibody-drug conjugates, retrograde transport allows STxB-conjugates to avoid degradation in lysosomes. STxB has furthermore a high stability against proteolytic degradation, the capacity to cross tissue barriers, and low immunogenicity in humans.²⁴⁻²⁵ Repeated administrations of STxB by the oral or intravenous route are well tolerated and do not cause adverse side effects.²⁰

All these properties make STxB a promising vector for imaging and targeted delivery in cancer treatment.²⁶ For

this purpose, an engineered variant of STxB (STxB-Cys), carrying an additional cysteine at the C-terminus, was developed²⁷ for its chemical conjugation with maleimide, isothiocyanate or sulfhydryl groups. The potential of STxB conjugates for imaging of Gb3 expressing solid tumors has already been demonstrated in mouse models of digestive cancer.^{13,20} The fluorescent dye fluorescein and a [¹⁸F]fluoropyridine radiotracer were chemically coupled to STxB-Cys.²⁸ Both conjugates accumulated at the tumor sites, allowing tumor visualization using confocal endoscopy and positron-emission tomography respectively. These imaging techniques however have limitations: optical fluorescence imaging is mainly restricted *in vivo* by limited depth of penetration (few cm) in tissue²⁹ while PET needs the production of a radionuclide labelled molecule (with a half-life of 110 min for ¹⁸F), and its spatial resolution is limited to about 1 mm for preclinical PET cameras, and to several mm for clinical PET cameras.³⁰ To circumvent these limitations, we considered magnetic resonance imaging as a promising technique to develop a molecular contrast agent for imaging of Gb3 expressing solid tumors.

MRI is a widespread whole body preclinical/clinical imaging technique, endowed with high spatial resolution (typical in plane resolution of about 100 μm for preclinical MRI and about 1 mm for clinical MRI). It is based on the detection of stable isotopes (mainly protons of water and fatty acid hydrogen atoms) and may be considered as the most flexible and multi-parametric anatomical and functional imaging technique. Discrimination between pathological and normal tissue with MRI may be optimized by the use of contrast agents. Gadolinium chelates are by far the most widely used contrastophores in clinical practice. They induce a local decrease of the longitudinal relaxation times T_1 of the water protons leading to contrast enhancement at the site of accumulation. The magnitude of this effect is given by equation 1. Where $1/T_1^0$ is the relaxation rate of the tissue without contrast agent, $[C]$ is the concentration of contrast agent within the tissue, and r_1 is the longitudinal relaxivity of the contrast agent.³¹⁻³²

$$1/T_1^{\text{obs}} = 1/T_1^0 + r_1 [C] \quad (1)$$

While conventional contrast-enhanced MRI yields mainly anatomical and physiological information, molecular MRI provides additional information at the molecular or cellular levels. It requires responsive or targeted probes specific of a biological process.³³⁻³⁴ In particular, conjugation of a contrastophore with a targeting moiety should enable detection of the conjugate and therefore the target *via* its effect on water proton relaxation times upon specific accumulation at the target site. However MRI suffers from rather low sensitivity and Gd(III) concentrations typically need to be in the micromolar range to be detectable.³⁵⁻³⁶ Such concentrations are rarely reached for biochemical targets and especially membrane receptors. Therefore, molecular MRI based on targeted contrast agents is still considered challenging.³⁷⁻⁴⁰ Recently, a peptidic MRI contrast agent (MT218) targeting overexpressed fibronectin in the stroma

of solid tumors⁴¹⁻⁴² received FDA approval for Phase 1 clinical trials.

Different systems were designed to achieve high concentration of contrastophores with high relaxivity at the site of interest. This goal may be pursued using nanoparticles, polymers, dendrimers, liposomes or microemulsion conjugating multiple contrastophores to the targeting moiety⁴³⁻⁴⁷ and/or taking advantage of receptor-mediated internalization to accumulate the targeted contrastophores.³⁷ Solid phase synthesis has been advantageously used for the development of complex and specific MRI probes.⁴⁸ Success of the strategy depends on accumulation of the vector-contrastophore conjugate at the cell-surface or inside the cell and therefore on its access to tumor cells, its affinity for the receptor, and the concentration of the receptor. If internalized, the intracellular trafficking pathway taken by the conjugates might have an effect since its trapping in a sub-cellular vesicle/endosome/lysosome can quench the expected relaxation rate gain⁴⁹⁻⁵⁰ and/or lead to the release of free toxic gadolinium.^{37,51} In this context, the STxB/Gb3 receptor system can be considered as a good candidate for the design of tumor cell targeted MRI contrast agents. It offers the possibility to directly address the contrastophores to the endoplasmic reticulum by circumventing acid-mediated endosomal-lysosomal degradation.⁵² To our knowledge, STxB has not yet been used for molecular MRI.

In the current paper we designed a potential tumor cell targeted imaging agent by conjugating each subunit of the STxB pentamer to a cyclotetradecapeptide platform carrying 9 monoamide DO₃A[Gd(III)] chelates. We measured the relaxivity of this conjugate, carrying theoretically up to 45 chelates, at 9.4 T and 1.5T. Its specific accumulation in Gb3 overexpressing HeLa cells was also quantified.

RESULTS AND DISCUSSION

Design and Synthesis

The MRI contrast agents were designed by the assembly of a contrastophore unit and a targeting moiety *via* a maleimide.

Contrastophore unit. We first considered the design and optimization of the contrastophore unit. It was built from a cyclic tetradecapeptide scaffold composed of an antiparallel β -sheet constrained by two β -turns and stabilized into a rigid conformation by intramolecular hydrogen bonds (Figure 1). This would limit the internal flexibility of the contrastophore and be favourable for its relaxivity.³⁸ This scaffold (named regioselectively addressable functionalized template) was originally developed by Mutter *et al.* in the 90's,³³ and presents two spatially independent domains in a constrained manner. Lysine (**19**) or diaminopropionic acid (**20**, **21**) side chains, oriented on one (**19**, **20**) or on both sides (**21**) of the scaffold, provide anchoring sites for six (**19**, **20**) or nine (**21**) monoamide DO₃A[Gd(III)]. One lysine side-chain on the scaffold remains at this stage protected with the

allyloxy carbonyl group, which was chosen for its high stability and its orthogonality in the solid phase peptide synthesis strategy used herein.⁵⁴ After Alloc cleavage, this lysine can be used to graft a maleimide derivative for the subsequent conjugation to STxB-Cys. The peptide scaffold advantageously ensures a constrained orientation of the side chains used to graft the monoamide DO₃A[Gd(III)].

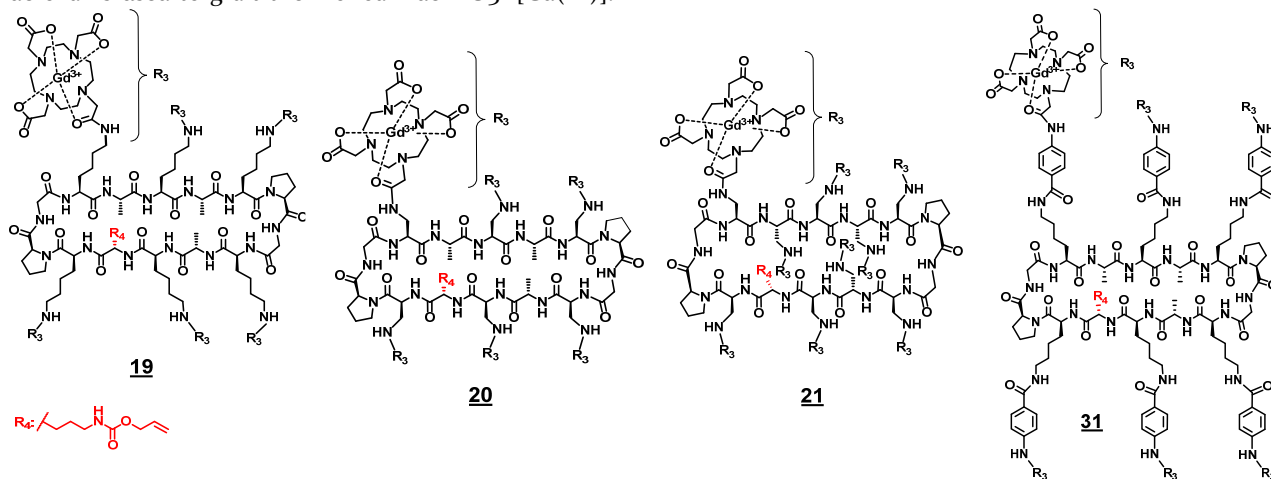


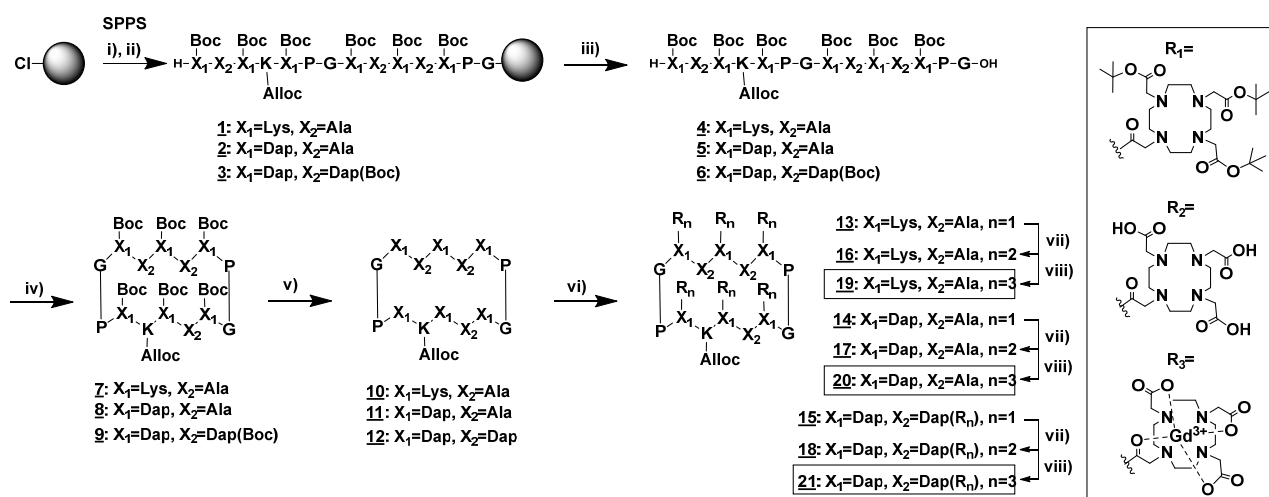
Figure 1. Chemical structures of cyclic peptide scaffolds **19** (six monoamide-DO₃A[Gd(III)] attached to the peptide scaffold by long length linkers), **20** (six monoamide-DO₃A[Gd(III)] attached to the peptide scaffold by short length linkers), **21** (nine monoamide-DO₃A[Gd(III)] attached to the peptide scaffold by short length linkers) and **31** (six monoamide-DO₃A[Gd(III)] attached to the peptide scaffold by linkers inducing π -stacking constraints).

A synthetic strategy in two steps was devised for compounds **19**, **20** and **21**: (1) SPPS of linear protected peptide fragments, followed by their cyclization in solution; (2) sequential deprotection-functionalization of amino acid side chains with 6 or 9 monoamide DO₃A[Gd(III)] complexes.

Compounds **19**, **20**, **21** and **31** (Figure 1) were designed to study the influence of: *i*) the length of the amino acid side chains linking the monoamide-DO₃A[Gd(III)] (**19** vs **20**), *ii*) the number of the gadolinium chelates (**20** vs **21**), and *iii*) π -stacking constraints (**19** vs **31**) on r_1 relaxivity of the contrastophore.

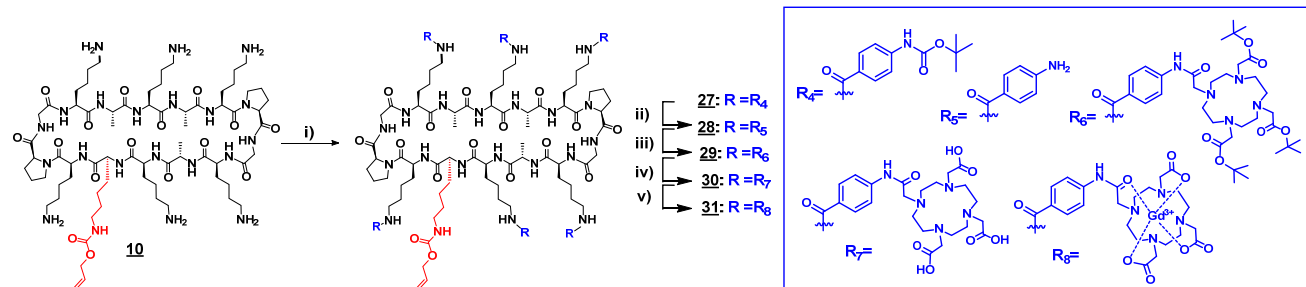
The acid-labile 2-chlorotrityl chloride resin was chosen to obtain the protected linear peptides **4**, **5** and **6** in a standard Fmoc/*t*Bu solid-phase chemistry (Scheme 1).⁵⁵ After nucleophilic substitution of the chloride on resin with Fmoc-Gly-OH and removal of the Fmoc group with 20 % piperidine in DMF, thirteen steps of Fmoc-AA-OH coupling/Fmoc removal were successively performed.

Scheme 1. Synthesis scheme of cyclic peptide scaffolds **19**, **20**, **21** functionalized with paramagnetic monoamide DO₃A[Gd(III)]



(i) Resin loading 0.8 mmol/g of resin, Fmoc-Gly-OH 2 equiv and DIPEA 3-4 equiv in CH₂Cl₂ (anhydrous) – Resin capping step: MeOH/DIPEA/CH₂Cl₂ (2/1/17 v/v/v) ; ii) SPPS: Coupling conditions: Fmoc-₁(AA)-OH 2 equiv, PyBOP 2 equiv and DIPEA 3-4 equiv in DMF - Deprotection conditions: 20 % piperidine in DMF; (iii) TFE/AcOH/CH₂Cl₂ (2/1/7 v/v/v); (iv) PyBOP 1.2 equiv and DIPEA 2-3 equiv in DMF ([linear peptide] 0.5 mM); (v) TFA/CH₂Cl₂ (1/1 v/v); (vi) DOTA-tris(*t*Bu)ester 1.5 equiv/NH₂, PyBOP 1.5 equiv/NH₂ and DIPEA 2-3 equiv/NH₂ in DMF; (vii) TFA/CH₂Cl₂ (1/1 v/v); (viii) GdCl₃ 2 equiv/monoamide DO₃A in aq. sol. (pH5).

Scheme 2. Synthesis scheme of cyclic peptide scaffold **31 functionalized with paramagnetic monoamide DO₃A[Gd(III)]**



(i) 4-(Boc-amino)benzoic acid 1.5 equiv/R₅, PyBOP 1.5 equiv/R₅ and DIPEA 3.8 equiv/R₅ in DMF; (ii) TFA/CH₂Cl₂ (1/1 v/v); (iii) DOTA-tris(*t*Bu)ester 3 equiv/R₆, HATU 3 equiv/R₆, TBTU 0.7 equiv/R₆, PyBOP 0.7 equiv/R₆ and DIPEA 8 equiv/R₆ in DMF (MW 75°C); (iv) TFA/CH₂Cl₂ (1/1 v/v); (v) GdCl₃ 3 equiv/R₇ in aq. acetate buffer (pH5).

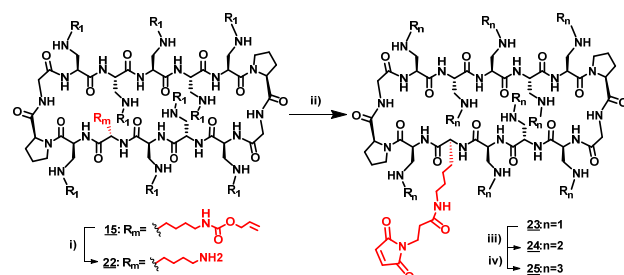
The coupling reactions were achieved under slightly basic conditions (pH 8-9) in DMF in the presence of DIPEA and using a 2-fold excess of both Fmoc-AA-OH and PyBOP. Cleavages of the peptides from the resin **1**, **2** and **3** were performed under mild acidic conditions to afford linear protected peptides **4**, **5** and **6**. The latter were then head-to-tail cyclized into the corresponding cyclopeptides **7**, **8** and **9** using PyBOP coupling reagent in DMF under high dilution condition as already reported.⁵³ When necessary, these cyclic peptides were purified by preparative reversed phase high-performance liquid chromatography. Removal of the Boc groups was achieved by treatment with TFA in CH₂Cl₂ (50/50 v/v) for 1 h to afford **10**, **11** and **12**. The deprotected amine of cyclic peptides **10**, **11** and **12** were then acylated with DOTA-tris(*t*Bu)ester under slightly basic conditions (pH 8-9 adjusted with DIPEA) using PyBOP as coupling reagent to provide **13**, **14** and **15**. Removal of the *t*Bu groups was achieved by treatment with TFA in CH₂Cl₂ (50/50 v/v) affording **16**, **17** and **18**. Gd(III) complexes were then formed by reacting these derivatized peptides with 2-fold excess of GdCl₃ per monoamide DO₃A in aqueous solution in the pH range 5-6 at room temperature. The cyclopeptides RAFT(monoamide DO₃A[Gd(III)])_n **19**, **20** and **21** were obtained with 34 to 55 % overall yield and over 95 % purity after purification by preparative RP-HPLC (Scheme 1).

In order to increase rotational constraint of the monoamide DO₃A[Gd(III)], we prepared the analogue **31** (Scheme 2) with a phenyl linker to induce π -stacking on the upper face of the cyclopeptide. Modifications of coupling protocols and longer reaction times proved necessary to get satisfying yields.

Maleimide derived contrastophore unit. The maleimide-derived contrastophore **25** was synthesized from the Alloc protected precursor **15**. First, the Alloc group was removed in neutral conditions with catalytic amounts of Pd(PPh₃)₄ in the presence of PhSiH₃ as a nucleophile to afford the desired amine derivatives **22** (Scheme 3).⁵⁴ The amine was then acylated with a 2-fold excess of 3-(maleimido)propionic acid NHS ester under slightly basic conditions (pH 8-9 adjusted with DIPEA) to provide

compound **23**. The removal of the *t*Bu groups was achieved by treatment with TFA in CH₂Cl₂ (50/50 v/v) and the complexation of monoamide DO₃A with GdCl₃ was performed in acetate buffer at pH 5 (0.1 M) to provide the functionalized contrastophore **25**. The low pH used for complexation prevented the hydrolysis of the maleimide group (Scheme 3).

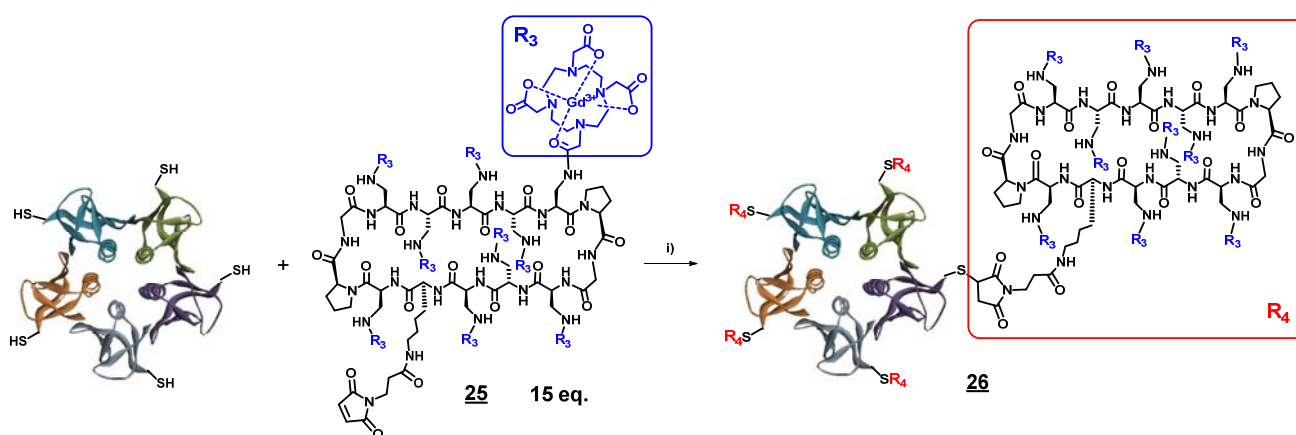
Scheme 3. Synthesis scheme of cyclic peptide scaffold **25 functionalized with paramagnetic monoamide DO₃A[Gd(III)] and maleimide**



(i) Pd(PPh₃)₄ 0.2 equiv, PhSiH₃ 100 equiv in CH₂Cl₂/DMF (3/1 v/v) (anhydrous) under argon; (ii) 3-(maleimido)propionic acid NHS ester 2 equiv and DIPEA 3 equiv (anhydrous) in CH₂Cl₂/DMF (1/1 v/v) (anhydrous) under argon; (iii) TFA/CH₂Cl₂ (1/1 v/v); (iv) GdCl₃ 2 equiv/moamide DO₃A in acetate buffer 0.1 M (pH 5). [R_n detailed in Scheme 1]

STxB-based targeted contrastophore unit. STxB-Cys and compound **25** were then conjugated through the thiol/maleimide reaction in aqueous conditions (PBS pH 7.4). STxB-Cys has the capacity to couple one molecule **25** per monomer with a maximal loading capacity of five molecules **25** per homopentamer. As seen by HPLC, the conjugation step proceeded cleanly and the reactions were almost complete after 48 h by using a 3-fold excess of compound **25** relative to each of the five thiol functions of STxB-Cys. Purification of conjugate **26** was performed by size-exclusion chromatography to remove compound **25** in excess. The STxB-[Gd(III)] conjugate **26** was obtained in PBS solution with a yield of 56 % after the purification step (Scheme 4).⁵⁶

Scheme 4. Synthesis scheme of STxB-based targeted MRI contrast agent **26 (STxB-[Gd(III)] conjugate)**



(i) PBS pH 7.4, 48 h.

Gd(III) quantification of conjugate **26 with ICP-MS.**

The amount of Gd(III) per STxB-conjugate **26** was measured by inductively coupled plasma mass spectrometry analysis.⁵⁷⁻⁵⁹ From this experiment, performed in triplicate, it appeared that the coupling of compound **25** in excess to STxB-Cys was not fully complete, leading to 4.3 ± 0.2 R_4 / STxB protein, corresponding to a mean of 39 Gd(III) per homopentamer (maximum loading: $5 R_4$) (detailed in supporting information).

Relaxivity. Relaxivity values for contrast agent (CA) compounds **19**, **20**, **31**, **21** (Figure 1), **25** (Scheme 3), **26** (Scheme 4) are given in Table 1. They were measured at 9.4 T and 1.5 T according to commonly used procedures as described in the material and methods section. Fitting of relaxation rates $R_1([CA])$ to the linear model for estimation of r_1 relaxivity was systematically excellent with determination coefficients $R^2 \approx 1$ (Figure 2).

Similarly, excellent fit quality was observed when fitting signal intensities $SI(TI)$ to the inversion recovery signal equation for T_1 estimation at 1.5 T.⁶⁰ This demonstrates the good quality of the acquired data. As examples, $SI(TI)$ graphs for **25** and **26** are given as supporting information (Figures S8). Experiments, i.e. compound synthesis, **Table 1. Relaxivity ($\text{mM}^{-1} \text{s}^{-1}$) of the multiplexed Gd(III)-MRI probes measured at 9.4 and 1.5 Tesla in water (or PBS for compound **26**)**

Compounds	Nb of Gd(III) per compound	MW	9.4 Tesla ^b		1.5 Tesla	
			r_1 per Gd(III)	r_1 per compound	r_1 per Gd(III)	r_1 per compound
DOTAREM [®]	1	557.6	3.0	3.0	2.9 ^c	2.9 ^c
19	6	4746.6	3.0	18.0	-	-
20	6	4494.1	3.8	23.0	-	-
31	6	5461.3	3.5	21.0	-	-
21	9	6161.0	3.6	32.1	-	-
25	9	6228.1	3.5	31.8	10.3 ^b	93.0 ^b
26	39 ^a	70099.0	3.9 [*]	150.2	12.2 ^{*b}	475.2 ^b

^a Experimental determination by ICP-MS measurement. ^b Measured at 22 °C. ^c Measured at 37 °C.⁶¹ ^{*}Based on the experimental determination of 39 Gd(III) per compound.

The r_1^{Gd} found at 9.4 T for all the compounds (Table 1) are in the range of those reported for $\text{DO}_3\text{A}[\text{Gd(III)}]$

sample preparations, and measurements, were performed once for each compound. Therefore, to estimate the overall precision of r_1 measurements, we consider r_1 per Gd(III) (r_1^{Gd}) of compounds **20**, **21**, **25** to be about equal due to very similar local molecular structures (Dap linker). Mean r_1^{Gd} and standard deviation for these compounds at 9.4 T are $3.63 \pm 0.15 \text{ mM}^{-1}\text{s}^{-1}$, consequently we assume an estimated maximum error of 5% on r_1 values. This measurement precision is similar to that given by Rohrer et al.⁶¹

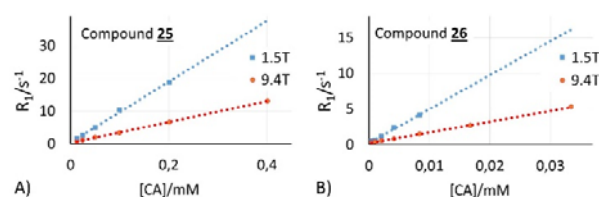


Figure 2. Relaxivity r_1 estimations at 9.4T and 1.5T. Representative examples of plots R_1 vs CA concentration fitted to a linear model. A) Compound **25**, $r_1 = (31.8 \pm 0.2) \text{ mM}^{-1}\text{s}^{-1}$ @ 9.4T, $r_1 = (93.0 \pm 2.5) \text{ mM}^{-1}\text{s}^{-1}$ @ 1.5T. B) Compound **26**, $r_1 = (150.2 \pm 1.5) \text{ mM}^{-1}\text{s}^{-1}$ @ 9.4T, $r_1 = (475.2 \pm 20.8) \text{ mM}^{-1}\text{s}^{-1}$ @ 1.5T.

multiplexed magnetic resonance probes at this field.^{45,62} It can be noticed that the r_1^{Gd} of compounds with short side

chain of Dap as linker (compounds **20**, **21**, **25**) are about 20 % higher than r_1^{Gd} of compound with a longer lysine side chain as linker (compound **19**). An 11% increase of r_1^{Gd} is also observed for compound **25** upon conjugation with the STxB protein (conjugate **26**). It is noteworthy that the r_1 value of $150 \text{ mM}^{-1}\text{s}^{-1}$ per conjugate for **26**, thanks to up to 45 Gd(III),⁶³ is higher than for most of the reported molecular targeted CA⁶⁴⁻⁶⁶ and lower than that of nanovectors bearing tens to hundreds of MRI contrastophores (inorganic nanoparticles, dendrimers...).⁶⁷⁻⁶⁸

Intracellular trafficking of STxB-targeted MRI contrast agent. STxB-targeted MRI contrast agent **26** was tested for its ability to be internalized into Gb₃-positive cells and to follow the retrograde trafficking route. Unmodified STxB-Cys or conjugate **26** were pre-incubated on HeLa cells for 30 min at 4 °C, a temperature at which only binding to the plasma membrane occurs since endocytosis is blocked. After several washes to remove

unbound STxB, the cells were incubated at 37 °C for 50 min for synchronized internalization, before fixation/permeabilization and immunolabelling of STxB and giantin, a Golgi-localized protein. Similarly to the unmodified STxB-Cys (Figure 3-A), the binding and trafficking of the conjugate **26** remain receptor specific (Figure 3-D), as shown by the absence of signal in HeLa cells treated with D,L-threo-1-phenyl-2-palmitoylamino-3-morpholino-1-propanol (PPMP), an inhibitor of glycosphingolipid biosynthesis (Figure 3-J).⁶⁹ Unmodified STxB-Cys (Figure 3A-C) as well as conjugate **26** (Figure 3D-F) colocalize with the Golgi. Despite the bulky gadolinium cargo, conjugate **26** thus appears to remain functional in terms of Gb₃ specificity and intracellular trafficking, circumventing endosomal-lysosomal degradation. In summary, the loading of up to 5 cyclic scaffolds, bearing nine monoamide DO₃A[Gd(III)] each, is compatible with the STxB targeting strategy and can be used for the design of targeted MRI contrast agent.

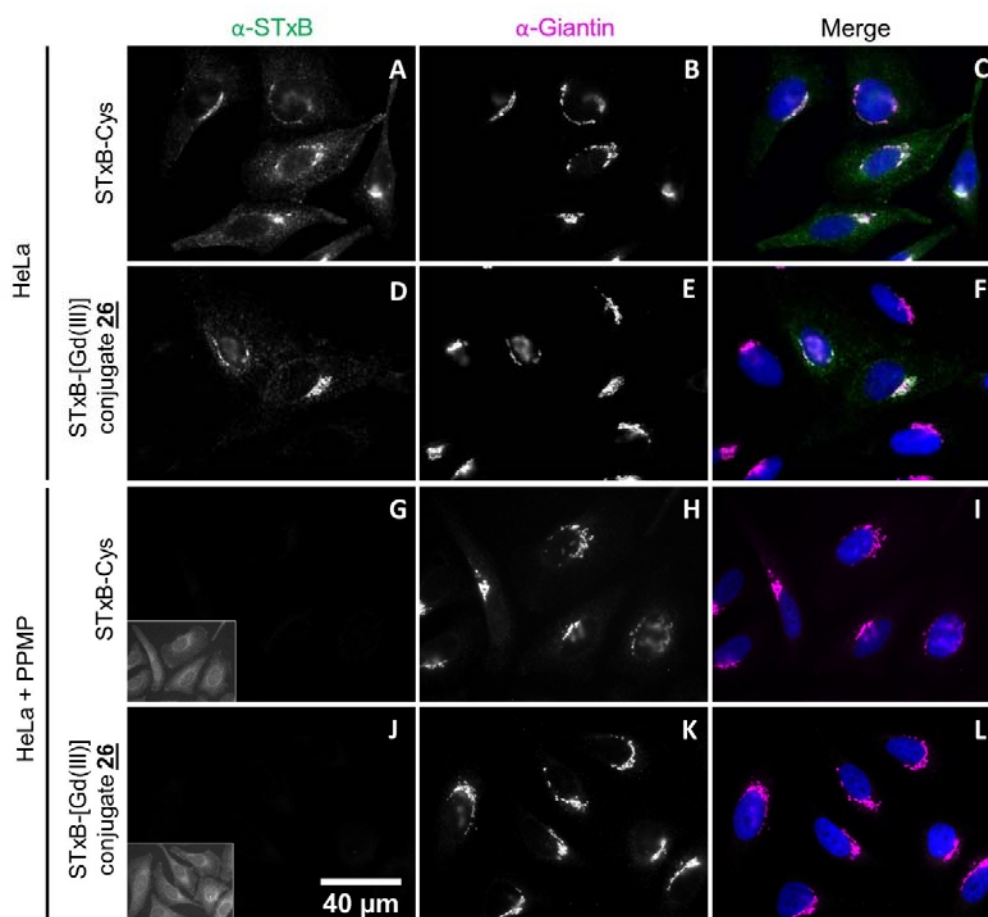


Figure 3. STxB-Cys and STxB-[Gd(III)] conjugate **26** intracellular trafficking. HeLa cells were incubated with 0.2 μM STxB-Cys or STxB-[Gd(III)] conjugate **26** (STxB monomer concentration) at 4 °C for 30 min, washed and incubated at 37 °C for 50 min, before fixation and labelling with the indicated antibodies anti-STxB (α-STxB) and anti-Giantin (α-Giantin: Golgi apparatus labelling). HeLa + PPMP (glycosphingolipid biosynthesis inhibitor): glycosphingolipid-negative control condition. Merge: Magenta – Giantin, Green – STxB, Blue – DNA stained with Hoechst. All microscopy pictures are shown with the same background and contrast parameters per channel. For PPMP treated conditions, the same picture with higher brightness and contrast parameters is also shown as a small insert in the bottom left corner. The signal detected is comparable to autofluorescence levels.

The relaxivity of final compounds, **25** and **26**, were also measured at a magnetic field of 1.5 T. As expected, for macromolecular agents with long rotational correlation time τ_R , r_1^{Gd} are higher at 1.5 T than at 9.4 T, with an about threefold increase for our compounds. At this typical clinical magnetic field, r_1 per conjugate of $475 \text{ mM}^{-1}\text{s}^{-1}$ is reached for the protein-based compound **26**.

Intracellular Gd(III) quantification with ICP-MS. The internalization capability of the STxB-based targeted contrast agent **26** was evaluated on a HeLa cell clone with homogeneous Gb₃ expression. Pre-treatment with PPMP provided Gb₃-negative HeLa cells for control. CHO cells (non-cancerous spontaneously immortalized ovary mammalian cell line) were used as a second Gb₃-negative control. The amounts of Gd(III) measured by ICP-MS in Gb₃-positive and negative cell pellets after 4 h incubation with **26** are given in Table 2.⁵⁸ From these measurements, intracellular Gd(III) concentration was estimated at $139 \mu\text{M}$ in Gb₃-positive cells. This is in accordance with theoretical estimation based on Gb₃ expression in HeLa cells. Indeed, given the number of STxB binding sites in HeLa cells, between 10^6 and 10^7 ,^{22,70-71} corresponding to STxB binding sites concentrations between 0.6 and $6 \mu\text{M}$,⁷² cellular Gd(III) concentrations (39 Gd(III) per STxB pentamer) may be roughly expected to be within the range of 23 to $234 \mu\text{M}$.

24% of the incubated STxB-[Gd(III)] conjugate **26** was internalized into Gb₃-positive cells, whereas Gd(III) was below detection limit in Gb₃-negative cells. These experiments confirmed the excellent specificity of STxB-conjugate for Gb₃ expressing cells and highlighted its capability to concentrate Gd(III) inside targeted cells. To our knowledge, these values exceed those reported for other targeted Gd(III)-conjugates and most Gd(III) formulations.^{67,73-74} They are well above the MRI detection limit for Gd(III) chelates estimated to be a few μM inside a voxel.^{35,75-76} For example, our estimated intracellular Gd(III) concentration in targeted cells is more than six times higher than that obtained with a prostate-specific membrane antigen targeted agent developed by Banerjee *et al.*⁶⁴ This estimated intracellular Gd(III) concentration is about tenfold above minimum detectable voxel concentration, which may be considered a safe margin for detectability as voxel concentration is expected to be lower depending on cell packing density or heterogeneous receptor expression *in vivo* in tumors.

Table 2. ICP-MS quantification of intracellular Gd(III) in HeLa cells (pre-treated or not with PPMP) and in CHO cells after incubation for 4 h at 37 °C with 0.2 μM STxB-[Gd(III)] conjugate **26 (STxB monomer concentration). Mean of three independent *in cellulo* experiments**

Cells	(Status)	Internalized Gd(III) / 10^6 cells	
		Amount (ng)	% ID ^a
HeLa	(Gb ₃ +)	65.4 ± 7	24.0
HeLa + PPMP	(Gb ₃ -)	< 0.25 (quantification limit)	< 0.1
CHO	(Gb ₃ -)	< 0.25 (quantification limit)	< 0.1

^a Mean incubated dose (ID = $272.2 \pm 13 \text{ ng}$ of incubated Gd(III) / 10^6 cells).

CONCLUSION

In summary, we developed a macromolecular targeted contrast agent, STxB-[Gd(III)] conjugate with up to 45 monoamide DO₃A[Gd(III)] for molecular MRI of an abundant cancer biomarker Gb₃. Rational design of this new targeted contrast agent resulted in a protein conjugate with a high r_1 relaxivity.

The STxB conjugate specifically binds Gb₃ expressing cancer cells and allows efficient intracellular Gd(III) accumulation, leading to a theoretically estimated and measured Gd(III) concentration higher than $100 \mu\text{M}$ in targeted cells, which should allow detection by MRI at preclinical as well as clinical magnetic fields. It needs now to be evaluated *in vivo* to confirm its potential for molecular imaging and to elaborate optimized measurement protocols.

MATERIALS AND METHODS

Materials. Protected amino acids were purchased from Iris Biotech GmbH (Germany), Bachem Biochimie SARL (France) or Novabiochem (Germany). PyBOP[®] was purchased from Novabiochem. 2-chlorotriylchloride[®] resin was obtained from Activotec (UK). Tri-*tert*-butyl 1,4,7,10-Tetraazacyclododecane-1,4,7,10-tetraacetate was purchased from TCI Europe (Belgium). Other reagents were obtained from Sigma-Aldrich (France) and Acros (France). Recombinant STxB-Cys was produced as previously described.⁷⁷ Its concentration and that of the STxB-[Gd(III)] conjugate **26** were determined by measuring absorbance at 280 nm of the solution with a Nanodrop 2000 (Thermo Scientific[™]) and using the approximated monomeric extinction coefficient $\epsilon=8370 \text{ M}^{-1}\text{cm}^{-1}$ calculated from Gill and von Hippel coefficients.⁷⁸

General methods of synthesis and characterization. If not specified, reactions were performed at room temperature, with synthesis grade solvents and not under specific atmosphere. RP-UPLC-MS analyses were performed on Waters equipment consisting of a Waters ACQUITY UPLC H-Class, a Waters PDA eLambda Detector (photodiode array detector) and a Waters SQ Detector 2 (ESI quadrupole mass spectrometer). The analytical column used was the ACQUITY UPLC BEH C₁₈ Column, 130\AA , $1.7 \mu\text{m}$, $2.1 \text{ mm} \times 50 \text{ mm}$ operated at $0.6 \text{ mL}\cdot\text{min}^{-1}$ with linear gradient programs in 2.5 min run time (classical program: 5 to 100 % of B in 2.5 min). UV monitoring was performed most of the time between 200-600 nm and was extracted at 214 nm. Solvent A consisted of H₂O containing 0.1 % (v/v) formic acid and solvent B was CH₃CN containing 0.1 % (v/v) FA. RP-HPLC purifications were performed on Waters equipment consisting of a Waters 2545 quaternary pump, a Waters 2998 photodiode array detector and Waters FlexInject manual injector module. The preparative column, XBridge BEH C₁₈ Column, 130\AA , $5 \mu\text{m}$, $4.6 \text{ mm} \times 150 \text{ mm}$ was operated at $30 \text{ mL}\cdot\text{min}^{-1}$ with linear gradient programs in 15 min run time. Solvent A consisted of H₂O containing 0.1 % (v/v) TFA and solvent B of CH₃CN containing 9.9 % (v/v) H₂O and 0.1 % TFA (classical focused programs: 10 % (v/v) slope of B in 15 min). Water was of Milli-Q quality and was obtained after

filtration of distilled water through a Milli-Q® cartridge system. CH₃CN, FA and TFA were of spectroscopic quality grade. The efficiency of RP-HPLC purifications to get rid of free gadolinium has been checked and confirmed by “xylenol test”.⁷⁹

Synthesis of cyclopeptide RAFT(monoamide DO₃A[Gd(III)])_n.

General procedure for solid-phase peptide synthesis. Assemblies of protected peptides **4**, **5** and **6** were carried out manually on 2-chlorotriylchloride® resin (theoretical loading of 0.84 mmol/g) using Fmoc/tBu strategy in a polypropylene reaction vessel fitted with a polyethylene frits.

Procedure A: loading of the first amino acid on the resin. The anchoring of the first amino acid (Fmoc-Gly-OH) through nucleophilic substitution was performed by stirring the resin in presence of 2 equiv of Fmoc-Gly-OH and 3-4 equiv of DIPEA in anhydrous CH₂Cl₂ (10 mL/g resin) for 30 min at room temperature, followed by a resin capping step with MeOH/DIPEA/CH₂Cl₂ (2/1/17 v/v/v) mixture (10.0 mL/g resin) for 10 min (repeated 2 times), to inactivate any remaining chlorotriyl function. The resin is then washed 3 times with DMF and once with CH₂Cl₂ (10.0 mL/g resin) for 1 min. The process yielded to an experimental resin loading around 0.50-0.60 mmol/g (determined by Fmoc dosage of the Fmoc removal solution (procedure B)).

Procedure B: Fmoc removal. N-α-Fmoc protecting groups was removed by stirring the resin in presence of a piperidine/DMF solution (1/4, v/v) (10.0 mL/g resin) for 10 min at room temperature.⁸⁰ The process was repeated 3 times, and the completeness of deprotection was verified by the UV absorption of the piperidine washings at 299 nm.⁸¹ The resin is then washed 5 times with DMF and once with CH₂Cl₂ (10.0 mL/g resin) for 1 min.

Procedure C: coupling steps. Coupling reactions were performed by stirring the resin in presence of 2 equiv of N-α-Fmoc-protected amino acid, 2 equiv of PyBOP and 3-4 equiv of DIPEA in DMF (10.0 mL/g resin) for 30 min at room temperature (equivalents are calculated from the experimental resin loading). The resin is then washed 3 times with DMF and once with CH₂Cl₂ (10.0 mL/g resin) for 1 min. Completeness of the coupling was controlled by TNBS test.⁸²

Procedure D: resin cleavage. The resins (**1**, **2** and **3**) were first washed 5 times with CH₂Cl₂ (10.0 mL/g resin) before stirring in 10.0 mL/g resin of a mixture of TFE/AcOH/CH₂Cl₂ (2/1/7 v/v/v) for 2 hours at room temperature and then filtrated. The resin is rinsed once with CH₂Cl₂ (10.0 mL/g resin) for 1 min. The recovered solutions were concentrated under reduced pressure, and white solid were obtained by precipitation, triturating and washing three times with diethyl ether. These crude linear peptides **4**, **5** and **6** were analyzed by RP-UPLC-MS and subsequently used without further purification.

H-Lys(Boc)-Ala-Lys(Boc)-Lys(Alloc)-Lys(Boc)-Pro-Gly-Lys(Boc)-Ala-Lys(Boc)-Ala-Lys(Boc)-Pro-Gly-OH (**4**). The product **4** was obtained as a white powder (0.50 g

of resin - Experimental loading: 0.55 mmol/g; 0.46 g, 0.21 mmol, 77 %). Analytical UPLC *t_r* = 2.30 min; ESI-MS (positive mode) calcd for C₉₉H₁₇₃N₂₁O₂₉ 2120.3, found *m/z* 2122.5 (M + H)⁺.

H-Dap(Boc)-Ala-Dap(Boc)-Lys(Alloc)-Dap(Boc)-Pro-Gly-Dap(Boc)-Ala-Dap(Boc)-Ala-Dap(Boc)-Pro-Gly-OH (**5**). The product **5** was obtained as a white powder (1.00 g of resin - Experimental loading: 0.53 mmol/g; 0.95 g, 0.49 mmol, 93 %). Analytical UPLC *t_r* = 2.17 min; ESI-MS (positive mode) calcd for C₈₁H₁₃₇N₂₁O₂₉ 1868.0, found *m/z* 1869.7 (M + H)⁺.

H-Dap(Boc)-Dap(Boc)-Dap(Boc)-Lys(Alloc)-Dap(Boc)-Pro-Gly-Dap(Boc)-Dap(Boc)-Dap(Boc)-Dap(Boc)-Dap(Boc)-Pro-Gly-OH (**6**). The product **6** was obtained as a white powder (1.00 g of resin - Experimental loading: 0.53 mmol/g; 1.20 g, 0.53 mmol, quant.). Analytical UPLC *t_r* = 2.40 min; ESI-MS (positive mode) calcd for C₉₆H₁₆₄N₂₄O₃₅ 2213.2, found *m/z* 2215.5 (M + H)⁺.

General procedure E: peptide cyclisation. Linear protected peptides **4**, **5** and **6** were dissolved in DMF (0.50 mM) with 2-3 equiv of DIPEA. PyBOP (1.2 equiv) was added, and the solutions were stirred at room temperature for 1 h. Solvent was removed under reduced pressure, and the residue was dissolved in the minimum of CH₂Cl₂. Diethyl ether was added to precipitate the peptide. Then it was triturated and washed 3 times with diethyl ether to yield crude material, if necessary, the latter was purified by preparative RP-HPLC (see general method and specific conditions for each compound).

c[Lys(Boc)-Ala-Lys(Boc)-Lys(Alloc)-Lys(Boc)-Pro-Gly-Lys(Boc)-Ala-Lys(Boc)-Ala-Lys(Boc)-Pro-Gly] (**7**). Starting from **4** (0.20 g, 0.09 mmol), the crude product **7** was obtained without purification as a white powder (0.19 g, 0.09 mmol, quant.). Analytical UPLC *t_r* = 2.76 min; ESI-MS (positive mode) calcd for C₉₉H₁₇₁N₂₁O₂₈ 2102.3, found *m/z* 2104.3 (M + H)⁺.

c[Dap(Boc)-Ala-Dap(Boc)-Lys(Alloc)-Dap(Boc)-Pro-Gly-Dap(Boc)-Ala-Dap(Boc)-Ala-Dap(Boc)-Pro-Gly] (**8**). Starting from **5** (0.20 g, 0.10 mmol), the purified product **8** was obtained as a white powder (0.13 g, 0.07 mmol, 67 %). Analytical UPLC *t_r* = 2.63 min; ESI-MS (positive mode) calcd for C₈₁H₁₃₅N₂₁O₂₈ 1850.0, found *m/z* 1851.9 (M + H)⁺. Preparative HPLC: focused gradient 60 to 70 % of B in 15 min.

c[Dap(Boc)-Dap(Boc)-Dap(Boc)-Lys(Alloc)-Dap(Boc)-Pro-Gly-Dap(Boc)-Dap(Boc)-Dap(Boc)-Dap(Boc)-Dap(Boc)-Dap(Boc)-Pro-Gly] (**9**). Starting from **6** (0.20 g, 0.09 mmol), the purified product **9** was obtained as a white powder (0.09 g, 0.04 mmol, 49 %). Analytical UPLC *t_r* = 2.95 min; ESI-MS (negative mode) calcd for C₉₆H₁₆₂N₂₄O₃₄ 2195.2, found *m/z* 2194.7 (M - H)⁻. Preparative HPLC: focused gradient 80 to 90 % of B in 15 min.

General procedure F: Boc and tBu Removals. Peptides were dissolved in TFA/CH₂Cl₂ (1/1 v/v) solution (10 mM), and the solutions were stirred at room temperature. Cyclic protected peptides **7**, **8** and **9** were stirred for 1 h for Boc removal. Solvent was removed under reduced pressure, and the residue was dissolved in the minimum of CH₂Cl₂.

Diethyl ether was added to precipitate the peptide. Then it was triturated and washed 3 times with diethyl ether to yield crude material. These crude peptides obtained as TFA salts **10**, **11** and **12** were analyzed by RP-UPLC-MS and subsequently used without further purification.

c[Lys-Ala-Lys-Lys(Alloc)-Lys-Pro-Gly-Lys-Ala-Lys-Ala-Lys-Pro-Gly] (10). Starting from **7** (0.19 g, 0.09 mmol), the crude product **10** was obtained as a white powder (0.20 g, 0.09 mmol, quant.). Analytical UPLC t_r = 0.33 min; ESI-MS (positive mode) calcd for $C_{69}H_{123}N_{21}O_{16}$ 1501.9, found m/z 1503.7 (M + H)⁺.

c[Dap-Ala-Dap-Lys(Alloc)-Dap-Pro-Gly-Dap-Ala-Dap-Ala-Dap-Pro-Gly] (11). Starting from **8** (0.13 g, 0.07 mmol), the crude product **11** was obtained as a white powder (0.12 g, 0.06 mmol, 95 %). Analytical UPLC t_r = 0.40 min; ESI-MS (positive mode) calcd for $C_{51}H_{87}N_{21}O_{16}$ 1249.7, found m/z 1251.3 (M + H)⁺.

c[Dap-Dap-Dap-Lys(Alloc)-Dap-Pro-Gly-Dap-Dap-Dap-Dap-Pro-Gly] (12). Starting from **9** (0.08 g, 0.04 mmol), the crude product **12** was obtained as a white powder (0.08 g, 0.04 mmol, quant.). Analytical UPLC t_r = 0.28 min; ESI-MS (positive mode) calcd for $C_{51}H_{90}N_{24}O_{16}$ 1294.7, found m/z 1296.6 (M + H)⁺.

*t*Bu removal of cyclic peptides **13**, **14** and **15** was performed according to the general procedure F with a stirring overnight to give the following crude products. The crude peptides **16**, **17** and **18** were analyzed by RP-UPLC-MS and subsequently used without further purification.

Compound 16. Starting from **13** (0.13 g, 0.03 mmol), the crude product **16** was obtained as a white powder (0.10 g, 0.03 mmol, quant.). Analytical UPLC t_r = 1.22 min; ESI-MS (positive mode) calcd for $C_{165}H_{279}N_{45}O_{58}$ 3819.0, found m/z 1274.8 (M + 3H)³⁺.

Compound 17. Starting from **14** (0.28 g, 0.06 mmol), the crude product **17** was obtained as a white powder (0.22 g, 0.06 mmol, quant.). Analytical UPLC t_r = 1.15 min; ESI-MS (positive mode) calcd for $C_{247}H_{243}N_{45}O_{58}$ 3566.7, found m/z 1190.7 (M + 3H)³⁺.

Compound 18. Starting from **15** (0.11 g, 0.02 mmol), the crude product **18** was obtained as a white powder (0.08 g, 0.02 mmol, 88 %). Analytical UPLC t_r = 0.64 min; ESI-MS (positive mode) calcd for $C_{195}H_{324}N_{60}O_{79}$ 4770.3, found m/z 1194.3 (M + 4H)⁴⁺.

General procedure G: DOTA-tris(tBu)ester conjugation to cyclic peptides. Cyclic peptide (**10**, **11** and **12**) was dissolved in DMF (10 mM) with DIPEA (2-3 equiv/NH₂). DOTA-tris(*t*Bu)ester (1.5 equiv/NH₂) and PyBOP (1.5 equiv/NH₂) were added. The solutions were stirred at room temperature from 1 h to overnight. Solvent was removed under reduced pressure, and the residue dissolved in the minimum of CH₂Cl₂. Diethyl ether was added to precipitate the peptide. Then it was triturated and washed 3 times with diethyl ether to yield crude material. The crude peptides **13**, **14** and **15** were analyzed by RP-UPLC-MS and subsequently used without further purification.

Compound 13. Starting from **10** (0.09 g, 0.05 mmol), the crude product **13** was obtained as a white powder (0.22 g,

0.05 mmol, quant.). Analytical UPLC t_r = 1.79 min; ESI-MS (positive mode) calcd for $C_{237}H_{423}N_{45}O_{58}$ 4828.1, found m/z 2416.5 (M + 2H)²⁺.

Compound 14. Starting from **11** (0.12 g, 0.06 mmol), the crude product **14** was obtained as a white powder (0.28 g, 0.06 mmol, quant.). Analytical UPLC t_r = 1.85 min; ESI-MS (positive mode) calcd for $C_{219}H_{387}N_{45}O_{58}$ 4575.9, found m/z 2290.3 (M + 2H)²⁺.

Compound 15. Starting from **12** (0.04 g, 0.02 mmol), the crude product **15** was obtained as a white powder (0.11 g, 0.02 mmol, quant.). Analytical UPLC t_r = 2.0 min; ESI-MS (positive mode) calcd for $C_{303}H_{540}N_{60}O_{79}$ 6284.0, found m/z 1573.1 (M + 4H)⁴⁺.

General procedure H: Gd(III) complexes formation. Cyclic deprotected conjugate **16**, **17** and **18** was dissolved in water (10 mM). The pH was adjusted to 5 by addition of a 1N aqueous solution of NaOH. GdCl₃ 2 equiv/monoamide DO3A in water (10 mM) was added by fraction. The pH was maintained to 5 by addition of a 1N aqueous solution of NaOH. The solution was then stirred at room temperature for 6 hours and was filtered on nylon filter (0.2 μm) before purification by preparative RP-HPLC (see general method and specific conditions for each compound).

Compound 19. Starting from **16** (0.10 g, 0.03 mmol), the purified product **19** was obtained as a white powder (0.03 g, 0.01 mmol, 25 %). Analytical UPLC t_r = 1.29 min; ESI-MS (positive mode) calcd for $C_{165}H_{261}GdN_{45}O_{58}$ 4748.4, found m/z 1583.6 (M + 3H)³⁺. Preparative HPLC: focused gradient 7 to 17 % of B in 15 min.

Compound 20. Starting from **17** (0.22 g, 0.06 mmol), the crude product **20** was obtained as a white powder (0.11 g, 0.03 mmol, 41 %). Analytical UPLC t_r = 1.40 min; ESI-MS (positive mode) calcd for $C_{147}H_{225}GdN_{45}O_{58}$ 4496.1, found m/z 1499.2 (M + 3H)³⁺. Preparative HPLC: focused gradient 5 to 15 % of B in 15 min.

Compound 21. Starting from **18** (0.08 g, 0.02 mmol), the crude product **21** was obtained as a white powder (0.04 g, 0.01 mmol, 37 %). Analytical UPLC t_r = 1.15 min; ESI-MS (positive mode) calcd for $C_{195}H_{297}GdN_{60}O_{79}$ 6164.4, found m/z 2055.0 (M + 3H)³⁺. Preparative HPLC: focused gradient 5 to 15 % of B in 15 min.

Procedure for 4-(Boc-amino)benzoic acid conjugation to cyclic peptide.

Compound 27. Cyclic deprotected peptide **10** (0.09 g, 0.04 mmol) was dissolved in DMF (10 mM). 4-(Boc-Amino)Benzoic Acid (0.09 g, 0.37 mmol, 1.5 equiv/R) and PyBOP (0.19 g, 0.37 mmol, 1.5 equiv/R) were added and the pH was adjusted to 8-9 by addition of DIPEA (0.16 mL, 0.94 mmol). The solution was stirred at room temperature for 2.5 h. Solvent was removed under reduced pressure, and the residue dissolved in the minimum of CH₂Cl₂/MeOH. Diethyl ether was added to precipitate the peptide. Then it was triturated and washed 3 times with diethyl ether to yield crude material. The crude product **27** was obtained as a white powder (0.12 g, 0.04 mmol, quant.). Analytical UPLC t_r = 1.23 min [focused gradient from 90 to 100 % of B

in 2.5 min]; ESI-MS (positive mode) calcd for $C_{141}H_{201}N_{27}O_{34}$ 2816.5, found m/z 1410.4 ($M + 2H$)²⁺.

Compound 28. The totality of cyclic protected peptide **27** was treated as described in the general procedure for Boc moiety removal before purification on preparative RP-HPLC column. The purified product **28** is obtained as a white powder (50.0 mg, 0.02 mmol, 41 % over two steps from peptide **10**). Analytical UPLC $t_r = 1.69$ min; ESI-MS (positive mode) calcd for $C_{111}H_{153}N_{27}O_{22}$ 2216.2, found m/z 740.1 ($M + 3H$)³⁺. Preparative HPLC: focused gradient from 20 to 30 % of B in 15 min.

Compound 29. Cyclic deprotected peptide **28** (0.05 g, 0.02 mmol) was dissolved in DMF (5 mM). Monoamide DO₃A-tris(*t*Bu)ester (0.23 g, 0.45 mmol, 4 equiv/R), HATU (0.13 g, 0.33 mmol, 3 equiv/R), TBTU (0.02 g, 0.07 mmol, 0.7 equiv/R) and PyBOP (0.04 g, 0.07 mmol, 0.7 equiv/R) were added and the pH was adjusted to 8-9 by addition of DIPEA. The solution was heated under microwaves at 75 °C for 6 h. Solvent was removed under reduced pressure, and the residue dissolved in the minimum of CH₂Cl₂. Diethyl ether was added to precipitate the peptide. Then it was triturated and washed 3 times with diethyl ether to yield crude material. The crude product **29** is obtained as a white powder (0.10 g, 0.02 mmol, quant.). Analytical UPLC $t_r = 1.73$ min; ESI-MS (positive mode) calcd for $C_{279}H_{453}N_{51}O_{64}$ 5542.4, found m/z 925.7 ($M + 6H$)⁶⁺.

Compound 30. The totality of cyclic protected peptide **29** was treated as described in the general procedure for *t*Bu moiety removal before purification on preparative RP-HPLC column. The purified product **30** was obtained as a white powder (15.0 mg, 3.00 μmol, 18 % over two steps from peptide **28**). Analytical UPLC $t_r = 1.35$ min; ESI-MS (positive mode) calcd for $C_{207}H_{309}N_{51}O_{64}$ 4533.2, found m/z 1135.1 ($M + 4H$)⁴⁺. Preparative HPLC: focused gradient 10 to 20 % of B in 15 min.

Compound 31. Cyclic deprotected peptide **30** (8.50 mg, 2.00 μmol) was dissolved in acetate buffer (0.6 mL; pH 5.4; 0.1 M) before addition of GdCl₃·H₂O (13 mg, 0.03 mmol, 3 equiv/R) in acetate buffer (0.4 mL; pH 5.4; 0.1 M) in two time. The solution was stirred at room temperature for 3 h, before purification on preparative RP-HPLC column. The purified product **31** is obtained as a white powder (7 mg, 1.3 μmol, 67 %). Analytical UPLC $t_r = 1.42$ min; ESI-MS (positive mode) calcd for $C_{207}H_{291}Gd_1N_{51}O_{64}$ 5462.6, found m/z 1093.2 ($M + 5H$)⁵⁺. Preparative HPLC: focused gradient 15 to 25 % of B in 15 min.

Synthesis of compound 22. The peptide **15** (0.11 g, 0.02 mmol) was dissolved in 2 mL of anhydrous CH₂Cl₂/DMF (3/1 v/v) under an argon atmosphere. Phenylsilane (0.22 mL, 1.80 mmol) and Pd(PPh₃)₄ (4 mg, 4 μmol) were added under an argon atmosphere and the reaction was stirred at room temperature for 30 min. The mixture was then treated with 0.50 mL of methanol before evaporation of the solvents under reduced pressure. The residue was dissolved in a minimum of CH₂Cl₂/MeOH (1/1 v/v), then precipitated, triturated and washed with diethyl ether to afford compound **22** as a slightly brown powder. This material was used without further purification. Analytical

UPLC $t_r = 1.86$ min; ESI-MS (positive mode) calcd for $C_{299}H_{536}N_{60}O_{77}$ 6284.0, found m/z 887.0 ($M + 7H$)⁷⁺.

Synthesis of compound 23. The totality of cyclic peptide **22** were dissolved in anhydrous CH₂Cl₂/DMF (1/1 v/v) (10 mM) with anhydrous DIPEA (20 μL, 0.12 mmol) under an argon atmosphere. 3-(maleimido)propionic acid *N*-hydroxysuccinimide ester (22 mg, 0.04 mol) were added. The solution was stirred at room temperature for 1 h. Solvent was removed under reduced pressure, and the residue was dissolved in the minimum of CH₂Cl₂. Diethyl ether was added to precipitate the peptide. Then it was triturated and washed 3 times with diethyl ether to yield crude material **23** as a slightly brown powder. This material was used without further purification. Analytical UPLC $t_r = 1.94$ min; ESI-MS (positive mode) calcd for $C_{306}H_{541}N_{61}O_{80}$ 6351.0, found m/z 909.1 ($M + 7H$)⁷⁺.

Synthesis of compound 24. The totality of peptide conjugates **23** was treated as described in the general procedure F with a stirring overnight before purification by preparative RP-HPLC to afford compound **24** as a white powder (0.03 g, 0.01, 32 % over 3 steps from peptide **15**). Analytical UPLC $t_r = 0.29$ min; ESI-MS (positive mode) calcd for $C_{198}H_{325}N_{61}O_{80}$ 4837.3, found m/z 1614.0 ($M + 3H$)³⁺. Preparative HPLC: focused gradient 3 to 20 % of B in 15 min.

Synthesis of compound 25. The cyclic peptide conjugates **24** (22.0 mg, 4.5 μmol) was treated as described in the general procedure H. The crude was purified by preparative RP-HPLC to afford the title product **25** as a white powder (15.0 mg, 2.4 μmol, 54 %). Analytical UPLC $t_r = 1.16$ min; ESI-MS (positive mode) calcd for $C_{198}H_{300}Gd_1N_{61}O_{80}$ 6230.4, found m/z 1557.0 ($M + 4H$)⁴⁺. Preparative HPLC: focused gradient 5 to 15 % of B in 15 min.

Synthesis of STxB-[Gd(III)] conjugate 26. Genetically engineered STxB-Cys, possessing five C-terminal cysteine residues was expressed and purified according to established procedures.⁷⁷ 3 equiv of cyclic peptide conjugates **25** (6.40 mg, 1.03 μmol) was added to STxB-Cys solution in PBS pH 7.4 (2.70 mg, 0.35 μmol, 6.1 mg/mL). The solution was stirred for 48 h at 21 °C (800 rpm). The conjugate **26** was purified on preparative SEC-LC column using AKTA pure chromatography system 25M on Sephadex 75 column (10-300GL) eluted with PBS at 0.5 mL/min affording 1,2 mL of uncolored pure solution of STxB-[Gd(III)] conjugate **26** at 2.30 mg/mL in PBS (2.76 mg, 0.20 μmol, 56 %). Analytical UPLC $t_r = 1.68$ min; ESI-MS (positive mode) calcd for $C_{540}H_{831}Gd_1N_{152}O_{189}S_4$ 14018.2, found m/z 1754.0 ($M + 8H$)⁸⁺ [data corresponding to STxB-Cys monomer]. ICP-MS Gd(III) quantification estimation of the substitution of the STxB protein by the cyclopeptide RAFT(monoamide DO₃A[Gd(III)])_n led to an effective functionalization of 4.3 ± 0.2 R₄ / STxB protein (*detailed in supporting information*).

ICP-MS quantification of Gd(III). The ICP-MS quantification of gadolinium contained in STxB-[Gd(III)] conjugate **26** solution or in cells was performed by the UT2A Company (Pau, France) on Agilent AT7800 instrument. The solution or cell pellets are placed in falcon

tubes and digested with 1 mL of nitric acid 70 % (JT Baker, Instra-analyzed), by sonication during 1 hour and placed at 85 °C during 2 hours on a regulated heating block and dilution at 10 mL with ultrapure water (Merck, Milli-Q). Isotopes ¹⁵⁵Gd and ¹⁵⁷Gd are measured. The instrument calibration is performed using 10 standard solutions prepared in nitric acid 2 % and included in the 0.01 to 10 µg/L range. If necessary, the extracts are diluted in the same HNO₃ 2 % matrix. Moreover, an internal standard, Rhodium, is added in each solution at 1 µg/L level to prevent from any deviation.

MRI r_1 relaxivity measurements. Relaxivity measurements were carried out at room temperature (around 22 °C) at two magnetic field strengths, at 9.4 T, a high preclinical research field, and at 1.5 T, a typical clinical field.

Relaxivity measurements at 9.4 T. Measurements were carried out on a microimaging system (Agilent Technologies, Santa Clara, CA, USA) equipped with a vertical WB magnet with 89 mm bore size, a 500 mT/m gradient system (BFG_73_55_100 RRI®) and a 40 mm inner diameter Millipede radiofrequency probe (Agilent). T₁ mapping was performed with a single slice inversion-recovery - Look-Locker imaging sequence under Vnmrj 4.0 Rev A (sequence name: gemsll, main parameters: TR = 7.38 ms; TE = 3.71 ms; TR(Inv) = 15 s; FA = 5°; MTX 128x128; Slth = 2 mm, pixel size = 0.39 x 0.39 mm²; 12 inversion times (TI) (s): 0.017, 0.05, 0.1, 0.5, 1, 2, 4, 6, 8, 10, 12, 14). Measurements were performed on compounds **19**, **20**, **21**, **25**, **26**, **31**. For each compound 6 samples with different concentrations were prepared by successive twofold dilution of a mother solution. Concentrations of aqueous mother solutions were similar for compounds **19**, **20**, **21**, **25**, **31** and ranged from 0.40 to 0.60 mM. For compound **26**, containing the protein, concentration of mother solution was 0.034 mM (in PBS pH 7.4). For T₁ mapping the samples (volume 200 µl) were transferred into six 5 mm i.d. NMR vials cylindrically arranged around a central water filled vial and imaging was performed on a central slice perpendicular to the vial axes. T₁ maps were computed by Vnmrj software, mean T₁ values measured inside circular regions of interest were used to compute relaxivity r_1 according to $R_1([CA]) = R_{10} + r_1 \cdot [CA]$, with $R_1 = 1/T_1$, $R_{10} = 1/T_{10}$ with T₁₀ being the value of T₁ for the solution without the CA, and [CA] being the concentration of the contrast agent compound. Fitting of $R_1([CA])$ to this linear model was performed using free SciDAVis 1.23 software (Scientific Data Analysis and Visualization).⁸³

Relaxivity measurements at 1.5 T. Measurements were carried out on a Philips Achieva clinical whole body scanner (Philips Healthcare, Best, The Netherlands). A clinical Head coil (SENSE_HEAD_8, Philips Healthcare) and an IR-Fast Spin Echo imaging sequence were used for T₁ mapping (main parameters: TR = 10 s; TE = 7.2 ms; Slth = 3 mm; MTX 232x74; pixel size = 0.45 x 0.45 mm²; 12 TI (s): 0.02, 0.05, 0.075, 0.1, 0.2, 0.3, 0.5, 1, 2, 3, 4, 5). Measurements were performed on compounds **25**, **26** (same samples as at 9.4 T). Eppendorf tubes containing the

samples were positioned in two rows (one for each compound) on a sample holder and imaging was performed on a horizontal slice passing through all samples. For the different inversion times mean signal intensities (SI) were measured inside circular regions of interest for the five samples with lowest concentration. T₁ values for each sample were obtained by fitting SI(TI) curves to the IR signal equation $(SI(TI) = SI_0 \cdot (1 - 2^{-b} \cdot \exp(-TI/T_1)))$ using SciDAVis software.⁶⁰ From these T₁ values, relaxivity r_1 was computed as described above. SI(TI) fits for compounds **25** and **26** are provided as supporting information (Figure S8).

Cell culture. The intracellular trafficking assay was done on HeLa cells, that were cultured at 37 °C under 5 % CO₂ in Dulbecco's modified Eagle's medium (DMEM, Invitrogen), supplemented with 10 % heat-inactivated fetal bovine serum, 0.01 % penicillin-streptomycin, 4 mM glutamine and 5 mM pyruvate. In the case of PPMP treatment (DL-threo-1-phenyl-2-palmitoylamino-3-morpholino-1-propanol, Enzo Life Sciences Inc.), HeLa cells were cultured for 6 days with 5 µM of compound before the experiment.

STxB-conjugate intracellular trafficking assay. Cells were plated the day before on lamellae in 4 well plate, 60 000 cells/well. Cells were incubated 30 min at 4 °C with 0.5 mL STxB dilution (STxB-Cys or STxB-[Gd(III)] conjugate **26**) at 0.20 µM (monomer concentration) in cold complete medium for binding on HeLa cells, pre-treated or not with PPMP. Then cells were washed 3 times to remove unbound STxB, before incubation at 37 °C for 50 min for synchronized internalization. Cells were then fixed in 4 % PFA in PBS for 15 min and permeabilized with saponine. Immunodetection was carried out using a primary mouse-monoclonal anti-STxB antibody (13C4), and a home-made rabbit polyclonal antibody against the Golgi marker giantin (Giantin is a Golgi protein), followed by detection thanks to appropriate fluorescently labelled secondary antibody. Slides were observed with material from the Cell and Tissue Imaging platform (PICT-IBiSA) of the Institut Curie: upright microscope Leica DM6000 with a camera CCD 1392x1040 CoolSnap HQ2 from Photometrics and illumination from a Lumen 200 lamp from Prior Scientific. 63x HCX Plan Apo objective was used for pictures.

Intracellular ICP-MS quantification of Gd(III). A subclone of HeLa cells, selected for their homogenous Gb3 expression, was either pre-treated or not with PPMP, and incubated at 37 °C for 4 h with STxB-[Gd(III)] conjugate **26** (0.2 µM monomeric concentration). After several washings to remove unbound and non-internalized conjugate **26**, cells were detached, counted, and recovered in pellet by centrifugation. The amount of Gd(III) present in each cell pellet was measured by ICP-MS analysis (*detailed in supporting information*).

ASSOCIATED CONTENT

Supporting Information

Characterization of new compounds (UPLC-UV chromatograms, mass spectrum), MS monitoring of the progress of the DOTA-tris(*t*Bu)ester coupling, ICP-MS Gd

quantification procedure, T₁ measurements at 1.5T on compounds **25** and **26** (PDF)
This material is available free of charge via the Internet at <http://pubs.acs.org>.

AUTHOR INFORMATION

Corresponding Author

* E-mail: stephanie.deville-foillard@cnrs.fr. Telephone: +33-1-69823059. Fax: +33-1-69823784.
<https://orcid.org/0000-0003-1902-4187>

Notes

The authors declare no competing financial interest.

ACKNOWLEDGMENT

The authors thank A. El Marjou (Protein Expression and Purification Core Facility), K. Niort, E. Dransart for their technical support for SEC purification, and the Cell & Tissue Imaging Platforms from Institut Curie (Paris). 1.5T MRI experiments were performed on the clinical MRI system owned by CNRS, Université Paris-Sud, and CEA, part of the imaging platform of CEA/SHFJ (Service Hospitalier Frédéric Joliot). The platform is affiliated to France Life Imaging (grant ANR-11-INBS-0006). This work was supported by Institut Curie, Institut des Substances Naturelles, CNRS and Université de Paris. This work received support from the grants ANR-11-LABX-0038, ANR-10-IDEX-0001-02 from Labex CeTisPhyBio and from ANR-10-IDEX-0001-02 PSL (Icx Paris Sciences et Lettres) and from "Frontières de l'Innovation en Recherche et Éducation" (FIRE) Doctoral School – Bettencourt Program.

ABBREVIATIONS

Ala, alanine; Alloc, allyloxycarbonyl; AcOH, acetic acid; Boc, *tert*-butoxycarbonyl; CA, contrast agents; Dap, diaminopropionic acid; DIPEA, *N,N*-diisopropylethylamine; DMF, *N,N*-dimethylformamide; DO₃A, 1,4,7,10-tetraazacyclododecane-1,4,7-triacetic acid; DOTA, 1,4,7,10-tetraazacyclododecane-1,4,7,10-tetraacetic acid; DNA, deoxyribonucleic acid; ESI, electrospray ionization; FA, formic acid; Fmoc, fluorenylmethoxycarbonyl; Gb₃, glycosphingolipid globotriaosyl ceramide; Gly, glycine; HATU, 1-[Bis(dimethylamino)methylene]-1*H*-1,2,3-triazolo[4,5-*b*]pyridinium 3-oxide hexafluorophosphate; HPLC, high performance liquid chromatography; ICP-MS, inductively coupled plasma mass spectrometry; IR, inversion recovery; Lys, lysine; NHS, *N*-hydroxysuccinimide; NMR, nuclear magnetic resonance; MRI, magnetic resonance imaging; MS, mass spectrometry; MW, microwaves; PBS, phosphate-buffered saline; PET, positron-emission tomography; PFA, paraformaldehyde; PMP, D,L-threo-1-phenyl-2-palmitoylamino-3-morpholino-1-propanol; Pro, proline; PyBOP, benzotriazole-1-yl-oxy-tris-pyrrolidino-phosphonium hexafluorophosphate; RAFT, regioselectively addressable functionalized templates; R₁, longitudinal relaxation rate; RP, reversed phase; SEC, size-exclusion chromatography; SI, signal intensity; SPPS, solid phase peptide synthesis; STxB, Shiga toxin B-subunit; *r*₁, longitudinal relaxivity of the contrast agent; TBTU, 2-(1*H*-Benzotriazole-1-yl)-1,1,3,3-tetramethylammonium tetrafluoroborate; *t*Bu, *tert*-butyl; TFA, trifluoroacetic acid; TFE, 2,2,2-trifluoroethanol; TI, inversion

time; TNBS, 2,4,6-trinitrobenzenesulfonic acid; *t*_r, retention time; UPLC, ultra performance liquid chromatography; UV, ultraviolet.

REFERENCES

- (1) Teng, F. F., Meng, X., Sun, X. D., and Yu, J. M. (2013) New strategy for monitoring targeted therapy: molecular imaging. *Int. J. Nanomedicine*. 8, 3703-3713.
- (2) O'Brien, A. D., Tesh, V. L., Donohue-Rolfe, A., Jackson, M. P., Olsnes, S., Sandvig, K., Lindberg, A. A., and Keusch, G. T. (1992) Shiga toxin: biochemistry, genetics, mode of action, and role in pathogenesis. *Curr. Top. Microbiol. Immunol.* 180, 65-94.
- (3) Proulx, F., Seidman, E. G., and Karpman, D. (2001) Pathogenesis of Shiga toxin-associated hemolytic uremic syndrome. *Pediatr. Res.* 50 (2), 163-171.
- (4) Pina, D. G., and Johannes, L. (2005) Cholera and Shiga toxin B-subunits: thermodynamic and structural considerations for function and biomedical applications. *Toxicon.* 45 (4), 389-393.
- (5) Ling, H., Boodhoo, A., Hazes, B., Cummings, M. D., Armstrong, G. D., Brunton, J. L., and Read, R. J. (1998) Structure of the shiga-like toxin I B-pentamer complexed with an analogue of its receptor Gb₃. *Biochemistry.* 37 (7), 1777-1788.
- (6) Engedal, N., Skotland, T., Torgersen, M. L., and Sandvig, K. (2011) Shiga toxin and its use in targeted cancer therapy and imaging. *Microb. Biotechnol.* 4 (1), 32-46.
- (7) Wiels, J., Fellous, M., and Tursz, T. (1981) Monoclonal antibody against a Burkitt lymphoma-associated antigen. *Proc. Natl. Acad. Sci. U. S. A.* 78 (10), 6485-6488.
- (8) Gordon, J., Mellstedt, H., Aman, P., Biberfeld, P., Bjorkholm, M., and Klein, G. (1983) Phenotypes in chronic B-lymphocytic leukemia probed by monoclonal antibodies and immunoglobulin secretion studies: identification of stages of maturation arrest and the relation to clinical findings. *Blood.* 62 (4), 910-917.
- (9) LaCasse, E. C., Bray, M. R., Patterson, B., Lim, W. M., Perampalam, S., Radvanyi, L. G., Keating, A., Stewart, A. K., Buckstein, R., Sandhu, J. S., Miller, N., Banerjee, D., Singh, D., Belch, A. R., Pilarski, L. M., and Garipey, J. (1999) Shiga-like toxin-1 receptor on human breast cancer, lymphoma, and myeloma and absence from CD34(+) hematopoietic stem cells: implications for ex vivo tumor purging and autologous stem cell transplantation. *Blood.* 94 (8), 2901-2910.
- (10) Johansson, D., Kosovac, E., Moharer, J., Ljuslinder, I., Brannstrom, T., Johansson, A., and Behnam-Motlagh, P. (2009) Expression of verotoxin-1 receptor Gb₃ in breast cancer tissue and verotoxin-1 signal transduction to apoptosis. *BMC Cancer.* 9, 67.
- (11) Arab, S., Russel, E., Chapman, W. B., Rosen, B., and Lingwood, C. A. (1997) Expression of the verotoxin receptor glycolipid, globotriaosylceramide, in ovarian hyperplasias. *Oncol. Res.* 9 (10), 553-563.
- (12) Distler, U., Souady, J., Hulsewig, M., Drmic-Hofman, I., Haier, J., Friedrich, A. W., Karch, H., Senninger, N., Dreisewerd, K., Berkenkamp, S., Schmidt, M. A., Peter-Katalinic, J., and Muthing, J. (2009) Shiga toxin receptor Gb₃Cer/CD77: tumor-association and promising therapeutic target in pancreas and colon cancer. *PLoS ONE.* 4 (8), e6813.
- (13) Falguieres, T., Maak, M., von Weyhern, C., Sarr, M., Sastre, X., Poupon, M. F., Robine, S., Johannes, L., and Janssen, K. P. (2008) Human colorectal tumors and metastases express Gb₃ and can be targeted by an intestinal pathogen-based delivery tool. *Mol. Cancer Ther.* 7 (8), 2498-2508.
- (14) Kovbasnjuk, O., Mourtazina, R., Baibakov, B., Wang, T., Elowsky, C., Choti, M. A., Kane, A., and Donowitz, M. (2005) The glycosphingolipid globotriaosylceramide in the metastatic transformation of colon cancer. *Proc. Natl. Acad. Sci. U. S. A.* 102 (52), 19087-19092.

- (15) Geyer, P. E., Maak, M., Nitsche, U., Perl, M., Novotny, A., Slotta-Huspenina, J., Dransart, E., Holtorf, A., Johannes, L., and Janssen, K. P. (2016) Gastric Adenocarcinomas Express the Glycosphingolipid Gb3/CD77: Targeting of Gastric Cancer Cells with Shiga Toxin B-Subunit. *Mol. Cancer Ther.* 15 (5), 1008-1017.
- (16) Ohyama, C., Fukushi, Y., Satoh, M., Saitoh, S., Orikasa, S., Nudelman, E., Straud, M., and Hakomori, S. (1990) Changes in glycolipid expression in human testicular tumor. *Int. J. Cancer.* 45 (6), 1040-1044.
- (17) Heath-Engel, H. M., and Lingwood, C. A. (2003) Verotoxin sensitivity of ECV304 cells in vitro and in vivo in a xenograft tumour model: VT1 as a tumour neovascular marker. *Angiogenesis.* 6 (2), 129-141.
- (18) Lingwood, C. A. (1999) Verotoxin/globotriaosyl ceramide recognition: angiopathy, angiogenesis and antineoplasia. *Biosci. Rep.* 19 (5), 345-354.
- (19) Viel, T., Dransart, E., Nemati, F., Henry, E., Theze, B., Decaudin, D., Lewandowski, D., Boisgard, R., Johannes, L., and Tavitian, B. (2008) In vivo tumor targeting by the B-subunit of shiga toxin. *Mol. Imaging.* 7 (6), 239-247.
- (20) Janssen, K. P., Vignjevic, D., Boisgard, R., Falguieres, T., Bousquet, G., Decaudin, D., Dolle, F., Louvard, D., Tavitian, B., Robine, S., and Johannes, L. (2006) In vivo tumor targeting using a novel intestinal pathogen-based delivery approach. *Cancer Res.* 66 (14), 7230-7236.
- (21) Johannes, L., and Romer, W. (2010) Shiga toxins--from cell biology to biomedical applications. *Nat. Rev. Microbiol.* 8 (2), 105-116.
- (22) Falguieres, T., Mallard, F., Baron, C., Hanau, D., Lingwood, C., Goud, B., Salamero, J., and Johannes, L. (2001) Targeting of Shiga toxin B-subunit to retrograde transport route in association with detergent-resistant membranes. *Mol. Biol. Cell.* 12 (8), 2453-2468.
- (23) Johannes, L., and Popoff, V. (2008) Tracing the retrograde route in protein trafficking. *Cell.* 135 (7), 1175-1187.
- (24) Levine, M. M., McEwen, J., Losonsky, G., Reymann, M., Harari, I., Brown, J. E., Taylor, D. N., Donohue-Rolfe, A., Cohen, D., Bennish, M., and et al. (1992) Antibodies to shiga holotoxin and to two synthetic peptides of the B subunit in sera of patients with Shigella dysenteriae 1 dysentery. *J. Clin. Microbiol.* 30 (7), 1636-1641.
- (25) Ludwig, K., Karmali, M. A., Sarkim, V., Bobrowski, C., Petric, M., Karch, H., Muller-Wiefel, D. E., and Arbeitsgemeinschaft fur Padiatrische, N. (2001) Antibody response to Shiga toxins Stx2 and Stx1 in children with enteropathic hemolytic-uremic syndrome. *J. Clin. Microbiol.* 39 (6), 2272-2279.
- (26) Luginbuehl, V., Meier, N., Kovar, K., and Rohrer, J. (2018) Intracellular drug delivery: Potential usefulness of engineered Shiga toxin subunit B for targeted cancer therapy. *Biotechnol. Adv.* 36 (3), 613-623.
- (27) Haicheur, N., Benchetrit, F., Amessou, M., Leclerc, C., Falguieres, T., Fayolle, C., Bismuth, E., Fridman, W. H., Johannes, L., and Tartour, E. (2003) The B subunit of Shiga toxin coupled to full-size antigenic protein elicits humoral and cell-mediated immune responses associated with a Th1-dominant polarization. *Int. Immunol.* 15 (10), 1161-1171.
- (28) de Bruin, B., Kuhnast, B., Hinnen, F., Yaouancq, L., Amessou, M., Johannes, L., Samson, A., Boisgard, R., Tavitian, B., and Dolle, F. (2005) 1-[3-(2-[18F]fluoropyridin-3-yloxy)propyl]pyrrole-2,5-dione: design, synthesis, and radiosynthesis of a new [18F]fluoropyridine-based maleimide reagent for the labeling of peptides and proteins. *Bioconjugate Chem.* 16 (2), 406-420.
- (29) Stuker, F., Ripoll, J., and Rudin, M. (2011) Fluorescence molecular tomography: principles and potential for pharmaceutical research. *Pharmaceutics.* 3 (2), 229-274.
- (30) Moses, W. W. (2011) Fundamental Limits of Spatial Resolution in PET. *Nucl. Instrum. Methods Phys. Res., A.* 648 Supplement 1, S236-S240.
- (31) Doan, B. T., Meme, M., and Beloeil, J. C. (2013) General Principles of MRI, in *The Chemistry of Contrast Agents in Medical Magnetic Resonance Imaging* (Merbach, A.; Helm, L.; Tóth, E., Eds.) pp 1-23, John Wiley & Sons, Ltd
- (32) Caravan, P., Ellison, J. J., McMurry, T. J., and Lauffer, R. B. (1999) Gadolinium(III) Chelates as MRI Contrast Agents: Structure, Dynamics, and Applications. *Chem. Rev.* 99 (9), 2293-2352.
- (33) Lacerda, S. (2018) Targeted Contrast Agents for Molecular MRI. *Inorganics.* 6 (4), 129.
- (34) Koudrina, A., and DeRosa, M. C. (2020) Advances in Medical Imaging: Aptamer- and Peptide-Targeted MRI and CT Contrast Agents. *ACS Omega.* 5 (36), 22691-22701.
- (35) Alvares, R. D. A., Szulc, D. A., and Cheng, H. M. (2017) A scale to measure MRI contrast agent sensitivity. *Sci. Rep.* 7 (1), 15493.
- (36) Zhou, Z., Qutaish, M., Han, Z., Schur, R. M., Liu, Y., Wilson, D. L., and Lu, Z. R. (2015) MRI detection of breast cancer micrometastases with a fibronectin-targeting contrast agent. *Nat. Commun.* 6, 7984.
- (37) Sim, N., and Parker, D. (2015) Critical design issues in the targeted molecular imaging of cell surface receptors. *Chem. Soc. Rev.* 44 (8), 2122-2134.
- (38) Wahsner, J., Gale, E. M., Rodriguez-Rodriguez, A., and Caravan, P. (2019) Chemistry of MRI Contrast Agents: Current Challenges and New Frontiers. *Chem. Rev.* 119 (2), 957-1057.
- (39) Villaraza, A. J., Bumb, A., and Brechbiel, M. W. (2010) Macromolecules, dendrimers, and nanomaterials in magnetic resonance imaging: the interplay between size, function, and pharmacokinetics. *Chem. Rev.* 110 (5), 2921-2959.
- (40) Li, H., and Meade, T. J. (2019) Molecular Magnetic Resonance Imaging with Gd(III)-Based Contrast Agents: Challenges and Key Advances. *J. Am. Chem. Soc.* 141 (43), 17025-17041.
- (41) Ayat, N. R., Qin, J. C., Cheng, H., Roelle, S., Gao, S., Li, Y., and Lu, Z. R. (2018) Optimization of ZD2 Peptide Targeted Gd(HP-DO3A) for Detection and Risk-Stratification of Prostate Cancer with MRI. *ACS Med. Chem. Lett.* 9 (7), 730-735.
- (42) Qiao, P., Ayat, N. R., Vaidya, A., Gao, S., Sun, W., Chou, S., Han, Z., Gilmore, H., Winter, J. M., and Lu, Z. R. (2020) Magnetic Resonance Molecular Imaging of Extradomain B Fibronectin Improves Imaging of Pancreatic Cancer Tumor Xenografts. *Front. Oncol.* 10, 586727.
- (43) Caravan, P., and Zhang, Z. (2013) Targeted MRI contrast agents, in *The chemistry of contrast agents in medical magnetic resonance imaging* (Merbach, A.; Helm, L.; Tóth, E., Eds.) pp 311-342, John Wiley & Sons, Ltd.
- (44) Ray, S., Li, Z., Hsu, C. H., Hwang, L. P., Lin, Y. C., Chou, P. T., and Lin, Y. Y. (2018) Dendrimer- and copolymer-based nanoparticles for magnetic resonance cancer theranostics. *Theranostics.* 8 (22), 6322-6349.
- (45) Mastarone, D. J., Harrison, V. S., Eckermann, A. L., Parigi, G., Luchinat, C., and Meade, T. J. (2011) A modular system for the synthesis of multiplexed magnetic resonance probes. *J. Am. Chem. Soc.* 133 (14), 5329-5337.
- (46) Boros, E., Gale, E. M., and Caravan, P. (2015) MR imaging probes: design and applications. *Dalton Trans.* 44 (11), 4804-4818.
- (47) Caravan, P., and Zhang, Z. (2012) Structure - relaxivity relationships among targeted MR contrast agents. *Eur. J. Inorg. Chem.* 2012 (12), 1916-1923.

- (48) Connah, L., and Angelovski, G. (2020) Solid phase synthesis in the development of magnetic resonance imaging probes. *Organic Chemistry Frontiers*. 7 (24), 4121-4141.
- (49) Terreno, E., Geninatti Crich, S., Belfiore, S., Biancone, L., Cabella, C., Esposito, G., Manazza, A. D., and Aime, S. (2006) Effect of the intracellular localization of a Gd-based imaging probe on the relaxation enhancement of water protons. *Magn. Reson. Med.* 55 (3), 491-497.
- (50) Aime, S., Castelli, D. D., Crich, S. G., Gianolio, E., and Terreno, E. (2009) Pushing the sensitivity envelope of lanthanide-based magnetic resonance imaging (MRI) contrast agents for molecular imaging applications. *Acc. Chem. Res.* 42 (7), 822-831.
- (51) Di Gregorio, E., Gianolio, E., Stefania, R., Barutello, G., Digilio, G., and Aime, S. (2013) On the fate of MRI Gd-based contrast agents in cells. Evidence for extensive degradation of linear complexes upon endosomal internalization. *Anal. Chem. (Wash.)*. 85 (12), 5627-5631.
- (52) Fraum, T. J., Ludwig, D. R., Bashir, M. R., and Fowler, K. J. (2017) Gadolinium-based contrast agents: A comprehensive risk assessment. *J. Magn. Reson. Imaging*. 46 (2), 338-353.
- (53) Dumy, P., Eggleston, I. M., Cervigni, S., Sila, U., Sun, X., and Mutter, M. (1995) A convenient synthesis of cyclic peptides as regioselectively addressable functionalized templates (RAFT). *Tetrahedron Lett.* 36 (8), 1255-1258.
- (54) Thieriet, N., Alsina, J., Giralt, E., Guibé, F., and Albericio, F. (1997) Use of Alloc-amino acids in solid-phase peptide synthesis. Tandem deprotection-coupling reactions using neutral conditions. *Tetrahedron Lett.* 38 (41), 7275-7278.
- (55) Foillard, S., Sancey, L., Coll, J. L., Boturyn, D., and Dumy, P. (2009) Targeted delivery of activatable fluorescent proapoptotic peptide into live cells. *Org. Biomol. Chem.* 7 (2), 221-224.
- (56) Protein conjugate amount determined by measuring absorbance at 280 nm of the solution (detailed in *Materials and Methods*).
- (57) Houk, R. S., Fassel, V. A., Flesch, G. D., Svec, H. J., Gray, A. L., and Taylor, C. E. (1980) Inductively coupled argon plasma as an ion source for mass spectrometric determination of trace elements. *Anal. Chem. (Wash.)*. 52 (14), 2283-2289.
- (58) Frame, E. M., and Uzgiris, E. E. (1998) Gadolinium determination in tissue samples by inductively coupled plasma mass spectrometry and inductively coupled plasma atomic emission spectrometry in evaluation of the action of magnetic resonance imaging contrast agents. *Analyst (Cambridge, U. K.)*. 123 (4), 675-679.
- (59) Strzeminska, I., Factor, C., Robert, P., Grindel, A. L., Comby, P. O., Szpunar, J., Corot, C., and Lobinski, R. (2020) Long-Term Evaluation of Gadolinium Retention in Rat Brain After Single Injection of a Clinically Relevant Dose of Gadolinium-Based Contrast Agents. *Invest. Radiol.* 55 (3), 138-143.
- (60) Stikov, N., Boudreau, M., Levesque, I. R., Tardif, C. L., Barral, J. K., and Pike, G. B. (2015) On the accuracy of T1 mapping: searching for common ground. *Magn. Reson. Med.* 73 (2), 514-522.
- (61) Rohrer, M., Bauer, H., Mintorovitch, J., Requardt, M., and Weinmann, H. J. (2005) Comparison of magnetic properties of MRI contrast media solutions at different magnetic field strengths. *Invest. Radiol.* 40 (11), 715-724.
- (62) Ndiaye, M., Malytskyi, V., Vangijzegem, T., Sauvage, F., Wels, M., Cadiou, C., Moreau, J., Henoumont, C., Boutry, S., Muller, R. N., Harakat, D., Smedt, S., Laurent, S., and Chuburu, F. (2019) Comparison of MRI Properties between Multimeric DOTAGA and DO3A Gadolinium-Dendron Conjugates. *Inorg. Chem.* 58 (19), 12798-12808.
- (63) Maximal theoretical gadolinium loading of STxB protein after conjugation with compound **25**.
- (64) Banerjee, S. R., Ngen, E. J., Rotz, M. W., Kakkad, S., Lisok, A., Pracitto, R., Pullambhatla, M., Chen, Z., Shah, T., Artemov, D., Meade, T. J., Bhujwala, Z. M., and Pomper, M. G. (2015) Synthesis and Evaluation of Gd(III)-Based Magnetic Resonance Contrast Agents for Molecular Imaging of Prostate-Specific Membrane Antigen. *Angew. Chem., Int. Ed.* 54 (37), 10778-10782.
- (65) Caravan, P., Farrar, C. T., Frullano, L., and Uppal, R. (2009) Influence of molecular parameters and increasing magnetic field strength on relaxivity of gadolinium- and manganese-based T1 contrast agents. *Contrast Media Mol. Imaging*. 4 (2), 89-100.
- (66) De Leon-Rodriguez, L. M., Lubag, A., Udugamasooriya, D. G., Proneth, B., Brekken, R. A., Sun, X., Kodadek, T., and Dean Sherry, A. (2010) MRI detection of VEGFR2 in vivo using a low molecular weight peptoid-(Gd)8-dendron for targeting. *J. Am. Chem. Soc.* 132 (37), 12829-12831.
- (67) Moore, L. K., Caldwell, M. A., Townsend, T. R., MacRenaris, K. W., Moyle-Heyrman, G., Rammohan, N., Schonher, E. K., Burdette, J. E., Ho, D., and Meade, T. J. (2019) Water-Soluble Nanoconjugate for Enhanced Cellular Delivery of Receptor-Targeted Magnetic Resonance Contrast Agents. *Bioconjugate Chem.* 30 (11), 2947-2957.
- (68) Bryant, L. H., Jr., Brechbiel, M. W., Wu, C., Bulte, J. W., Herynek, V., and Frank, J. A. (1999) Synthesis and relaxometry of high-generation (G = 5, 7, 9, and 10) PAMAM dendrimer-DOTA-gadolinium chelates. *J. Magn. Reson. Imaging*. 9 (2), 348-352.
- (69) Abe, A., Inokuchi, J., Jimbo, M., Shimeno, H., Nagamatsu, A., Shayman, J. A., Shukla, G. S., and Radin, N. S. (1992) Improved inhibitors of glucosylceramide synthase. *J. Biochem., Tokyo*. 111 (2), 191-196.
- (70) Johannes, L., Tenza, D., Antony, C., and Goud, B. (1997) Retrograde transport of KDEL-bearing B-fragment of Shiga toxin. *J. Biol. Chem.* 272 (31), 19554-19561.
- (71) Falguieres, T., Romer, W., Amessou, M., Afonso, C., Wolf, C., Tabet, J. C., Lamaze, C., and Johannes, L. (2006) Functionally different pools of Shiga toxin receptor, globotriaosyl ceramide, in HeLa cells. *FEBS J.* 273 (22), 5205-5218.
- (72) Average volume of HeLa cell is 3000 μm^3 (R. Milo et al., *Cell Biology by the Numbers*, Garland Science 2016).
- (73) Rammohan, N., Holbrook, R. J., Rotz, M. W., MacRenaris, K. W., Preslar, A. T., Carney, C. E., Reichova, V., and Meade, T. J. (2017) Gd(III)-Gold Nanoconjugates Provide Remarkable Cell Labeling for High Field Magnetic Resonance Imaging. *Bioconjugate Chem.* 28 (1), 153-160.
- (74) Vistain, L. F., Rotz, M. W., Rathore, R., Preslar, A. T., and Meade, T. J. (2016) Targeted delivery of gold nanoparticle contrast agents for reporting gene detection by magnetic resonance imaging. *Chem. Commun. (Cambridge, U. K.)*. 52 (1), 160-163.
- (75) Verma, K. D., Massing, J. O., Kamper, S. G., Carney, C. E., MacRenaris, K. W., Basilion, J. P., and Meade, T. J. (2017) Synthesis and evaluation of MR probes for targeted-reporter imaging. *Chem. Sci.* 8 (8), 5764-5768.
- (76) Hanaoka, K., Lubag, A. J. M., Castillo-Muzquiz, A., Kodadek, T., and Sherry, A. D. (2008) The detection limit of a Gd³⁺-based T1 agent is substantially reduced when targeted to a protein microdomain. *Magn. Reson. Imaging*. 26 (5), 608-617.
- (77) Mallard, F., and Johannes, L. (2003) Shiga toxin B-subunit as a tool to study retrograde transport. *Methods Mol. Med.* 73, 209-220.
- (78) Gill, S. C., and von Hippel, P. H. (1989) Calculation of protein extinction coefficients from amino acid sequence data. *Anal. Biochem.* 182 (2), 319-326.
- (79) Barge, A., Cravotto, G., Gianolio, E., and Fedeli, F. (2006) How to determine free Gd and free ligand in solution of Gd chelates. A technical note. *Contrast Media Mol. Imaging*. 1 (5), 184-188.
- (80) Atherton, E., Fox, H., Harkiss, D., Logan, C. J., Sheppard, R. C., and Williams, B. J. (1978) A mild procedure for solid phase

peptide synthesis: use of fluorenylmethoxycarbonylamino-acids. *J. Chem. Soc., Chem. Commun.* (13), 537-539.

(81) Meienhofer, J., Waki, M., Heimer, E. P., Lambros, T. J., Makofske, R. C., and Chang, C. D. (1979) Solid phase synthesis without repetitive acidolysis. *Int. J. Pept. Protein Res.* 13 (1), 35-42.

(82) Hancock, W. S., and Battersby, J. E. (1976) A new micro-test for the detection of incomplete coupling reactions in solid-phase peptide synthesis using 2,4,6-trinitrobenzenesulphonic acid. *Anal. Biochem.* 71 (1), 260-264.

(83) <http://scidavis.sourceforge.net/>.

